Elemental analysis of Oxygenated Organic Coating on Black Carbon Particles using a Soot-Particle Aerosol Mass Spectrometer

Mutian Ma[1], Laura-Hélèna Rivellini[2], YuXi Cui[1], Megan D. Willis[3], Rio Wilkie[4], Jonathan P. D. Abbatt[4], Manjula R. Canagaratna[5], Junfeng Wang[6], Xinlei Ge[6], Alex K.Y. Lee[1,2]

[1] Department of Civil and Environmental Engineering, National University of Singapore, Singapore

[2] NUS Environmental Research Institute, National University of Singapore, Singapore

[3] Lawrence Berkeley National Lab, Chemical Sciences Division, Berkeley, CA, USA

[4] Department of Chemistry, University of Toronto, Toronto, ON, Canada

[5] Aerodyne Research, Inc., Billerica, MA, USA

[6] School of Environmental Science and Engineering, Nanjing University of Information Science and Technology, Nanjing, China

Correspondence to: Alex K. Y. Lee (ceelkya@nus.edu.sg)

Table S1. Summary of elemental ratios and time series correlation of PMF factors based on co-located measurements in Beijing summer (Xie et al., 2019a; Xu et al., 2019), Beijing winter (Wang et al., 2019; Xie et al., 2019b), California Research at the Nexus of Air Quality and Climate Change (CalNex) 2010 campaign (Massoli et al., 2015), Fontana, CA (Chen et al., 2018; Lee et al., 2017), and Tibet (Wang et al., 2017; Xu et al., 2018).

Location / Campaign	HR-ToF-AMS				SP-AMS LV scheme[#]				R
	Study	PMF factor	H:C	O:C	Study	PMF factor	H:C	O:C	
Beijing summer	Xie et al. (2019a)	LO-OOA	1.34	0.49	Xu et al. (2019)	LO-OOA	1.6	0.28	0.88
Beijing winter	Xie et al. (2019b)	LO-OOA	1.61	0.6	Wang et al. (2019)	OOA1	1.55	0.37	0.92
Beijing winter	Xie et al. (2019b)	MO-OOA	1.36	0.97	Wang et al. (2019)	OOA2	1.57	1.23	0.97
CalNex	Massoli et al. (2015)	SV-OOA	1.58	0.54	Massoli et al. (2015)	SV-OOA	1.83	0.45	0.92
CalNex	Massoli et al. (2015)	LV-OOA	1.2	1.4	Massoli et al. (2015)	LV-OOA	1.4	1.16	0.84
Fontana, CA	Chen et al. (2018)	VOOA	0.78	1.4	Lee et al. (2017)	OOA2	1.63	0.63	0.76
Tibet	Xu et al. (2018)	MO-OOA	1.04	0.96	Wang et al. (2017)	BBOA	1.48	0.51	0.96

[#] The inter-conversion factors that were determined in this work, were applied for calculating H:C and O:C ratios.

Table S2. Summary of H:C, O:C and. OS_c determined by the SP-AMS 1

			True value			Tungsten vaporizer			Laser vaporizer		
Class	**Species**	**Formula**	**H:C**	**O:C**	**OSc**	**H:C**	**O:C**	**OSc**	**H:C**	**O:C**	**OSc**
Multifunctional	Citric acid	$C_6H_8O_7$	1.33	1.17	1.00	1.42	0.93	0.43	1.66	0.72	-0.21
Multifunctional	Glycolic acid	$C_2H_4O_3$	2.00	1.50	1.00	1.86	0.78	-0.31	1.71	0.53	-0.64
Multifunctional	Malic Acid	$C_4H_6O_5$	1.50	1.25	1.00	1.55	1.00	0.44	1.63	1.00	0.37
Multifunctional	Tartaric acid	$C_4H_6O_6$	1.50	1.50	1.50	1.48	1.34	1.20	1.63	1.52	1.40
Diacids	Adipic Acid	$C_6H_{10}O_4$	1.67	0.67	-0.33	1.71	0.60	-0.51	1.71	0.46	-0.79
Diacids	Azelaic Acid	$C_9H_{16}O_4$	1.78	0.44	-0.89	1.65	0.29	-1.07	1.90	0.35	-1.19
Diacids	Glutaric acid	$C_5H_8O_4$	1.60	0.80	0	1.64	0.44	-0.76	1.66	0.47	-0.71
Diacids	Malonic acid	$C_3H_4O_4$	1.33	1.33	1.33	1.36	1.12	0.87	1.61	1.10	0.59
Diacids	Oxalic acid	$C_2H_2O_4$	1.00	2.00	3.00	1.13	1.91	2.68	1.36	1.72	2.09
Diacids	Phthalic acid	$C_8H_6O_4$	0.75	0.50	0.25	0.84	0.26	-0.32	0.95	0.25	-0.46
Diacids	Pimelic acid	$C_7H_{12}O_4$	1.71	0.57	-0.57	1.66	0.42	-0.82	1.83	0.41	-1.02
Diacids	Suberic acid	$C_8H_{14}O_4$	1.75	0.50	-0.75	1.58	0.33	-0.93	1.85	0.40	-1.06
Diacids	Succinic acid	$C_4H_6O_4$	1.50	1.00	0.50	1.72	0.77	-0.18	1.48	0.83	0.17
Alcohols	Arabitol	$C_5H_{12}O_5$	2.4	1.00	-0.4	1.59	0.83	0.06	2.13	0.81	-0.51
Alcohols	Glucose	$C_6H_{12}O_6$	2.00	1.00	0	2.01	1.01	0.02	2.09	1.00	-0.10
Alcohols	Levoglucosan	$C_6H_{10}O_5$	1.67	0.83	0	1.85	0.77	-0.31	2.06	0.86	-0.33
Alcohols	Sucrose	$C_{12}H_{22}O_{11}$	1.83	0.92	0	1.90	0.900	-0.10	1.99	0.83	-0.32
Alcohols	Xylitol	$C_5H_{12}O_5$	2.40	1.00	-0.4	1.92	0.78	-0.37	2.21	0.90	-0.41

Table S3. Summary of H:C, O:C and. OS_c determined by the SP-AMS 2

			True value			Tungsten vaporizer			Laser vaporizer		
Species	**Class**	**Formula**	**H:C**	**O:C**	**OSc**	**H:C**	**O:C**	**OSc**	**H:C**	**O:C**	**OSc**
Cis-Pinonic acid	Multifunctional	$C_{10}H_{16}O_3$	1.60	0.30	-1.00	1.69	0.25	-1.19	0.48	1.30	-0.34
Citric acid	Multifunctional	$C_6H_8O_7$	1.33	1.17	1.00	1.40	1.00	0.59	0.94	1.39	0.49
Glutamic acid	Multifunctional	$C_5H_9NO_4$	1.80	0.80	-0.2		NA		0.29	2.03	-1.45
Glycolic acid	Multifunctional	$C_2H_4O_3$	2.00	1.50	1.00	1.45	1.24	1.04	0.65	1.56	-0.26
Levulinic acid	Multifunctional	$C_5H_8O_3$	1.60	0.60	-0.4		NA		1.00	1.81	0.19
Malic acid	Multifunctional	$C_4H_6O_5$	1.50	1.25	1.00	1.56	1.10	0.64	0.60	1.55	-0.35
Pyruvic acid	Multifunctional	$C_3H_4O_3$	1.33	1.00	0.67	1.32	0.74	0.15	1.52	1.94	1.10
Tartaric acid	Multifunctional	$C_4H_6O_6$	1.50	1.50	1.5	1.60	1.74	1.88	0.09	2.30	-2.12
Adipic acid	Diacids	$C_6H_{10}O_4$	1.67	0.67	-0.33	1.60	0.43	-0.74	0.46	1.87	-0.95
Azelaic acid	Diacids	$C_9H_{16}O_4$	1.78	0.44	-0.89	1.62	0.32	-0.99	0.32	1.94	-1.30
Glutaric acid	Diacids	$C_5H_8O_4$	1.6	0.80	0	1.46	0.57	-0.33	0.56	1.80	-0.68
Maleic acid	Diacids	$C_4H_4O_4$	1.00	1.00	1.00	1.56	1.10	0.64	0.65	1.34	-0.04
Malonic acid	Diacids	$C_3H_4O_4$	1.33	1.33	1.33	1.58	1.09	0.59	1.13	1.83	0.43
Oxalic acid	Diacids	$C_2H_2O_4$	1.00	2.00	3.00	0.92	2.42	3.92	1.68	1.34	2.02
Succinic acid	Diacids	$C_4H_6O_4$	1.50	1.00	0.50	1.64	0.50	-0.64	0.55	1.89	-0.79
Tricarballylic acid	Polyacids	$C_6H_8O_6$	1.33	1.00	0.67	1.30	0.65	-0.01	0.56	1.57	-0.45
1,5-Pentanediol	Alcohols	$C_5H_{12}O_2$	2.4	0.40	-1.6		NA		0.44	1.70	-0.82
Dextrose	Alcohols	$C_6H_{12}O_6$	2.00	1.00	0		NA		0.87	1.87	-0.13
Phenol	Alcohols	C_6H_6O	1.00	0.17	-0.67		NA		0.62	1.81	-0.57
Bis(2-ethylhexyl) Sebacate	Esters	$C_{26}H_{50}O_4$	1.92	0.15	-1.62		NA		0.1	2.23	-2.03

Table S4. Summary of H:C, O:C and. OS_c determined by the SP-AMS 3

			True value			Tungsten vaporizer			Laser vaporizer		
Species	**Class**	**Formula**	**H:C**	**O:C**	**OSc**	**H:C**	**O:C**	**OSc**	**H:C**	**O:C**	**OSc**
Cis-Pinonic Acid	Multifunctional	$C_{10}H_{16}O_3$	1.60	0.30	-1.00	1.43	0.22	-0.99	1.53	0.19	-1.15
Citric acid	Multifunctional	$C_6H_8O_7$	1.33	1.17	1.00	1.18	1.03	0.88	1.19	0.86	0.52
Ketoglutaric Acid	Multifunctional	$C_5H_6O_5$	1.20	1.00	0.80	1.20	0.84	0.48	1.44	0.54	-0.36
Ketopimelic acid	Multifunctional	$C_7H_{10}O_5$	1.43	0.71	0	1.10	0.57	0.04	1.39	0.42	-0.55
Tartaric acid	Multifunctional	$C_4H_6O_6$	1.50	1.50	1.50	1.40	1.51	1.62	1.66	1.55	1.43
Azelaic Acid	Diacids	$C_9H_{16}O_4$	1.78	0.44	-0.89	1.34	0.28	-0.78	1.59	0.23	-1.13
Glutaric acid	Diacids	$C_5H_8O_4$	1.60	0.80	0	1.34	0.46	-0.42	1.47	0.46	-0.54
Malonic acid	Diacids	$C_3H_4O_4$	1.33	1.33	1.33	1.24	1.12	1	1.39	0.91	0.43
Pimelic acid	Diacids	$C_7H_{12}O_4$	1.71	0.57	-0.57	1.30	0.34	-0.62	1.56	0.31	-0.94
Succinic acid	Diacids	$C_4H_6O_4$	1.50	1.00	0.50	1.57	0.51	-0.55	1.56	0.46	-0.65
Sucrose	Alcohols	$C_{12}H_{22}O_{11}$	1.83	0.92	0	1.86	0.6	-0.66	1.60	0.55	-0.50
Xylitol	Alcohols	$C_5H_{12}O_5$	2.40	1.00	-0.40	1.74	0.68	-0.38	1.87	0.63	-0.60

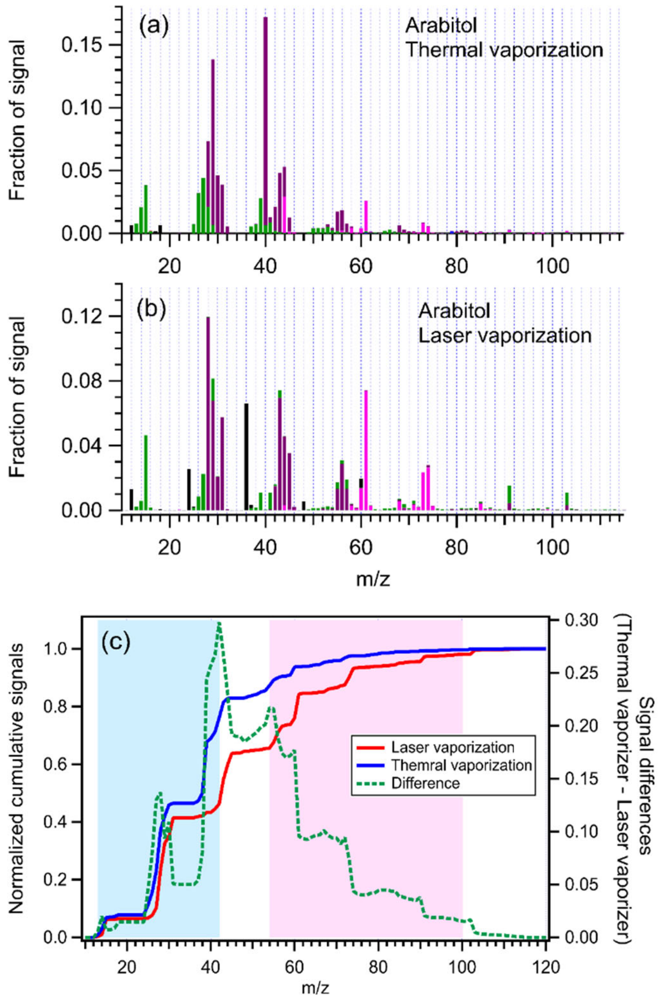

Figure S1. Mass spectra of arabitol, measured by the SP-AMS 1 using the tungsten (a) and laser (b) vaporization schemes. (c) Normalized cumulative histogram of mass-to-charge ratios for the oxygenated organic compounds measured by the SP-AMS 1. The blue area indicates that the thermal vaporization scheme tends to provide organic fragments with smaller m/z, whereas the red area indicates that the laser vaporization scheme tends to give organic fragments with larger m/z.

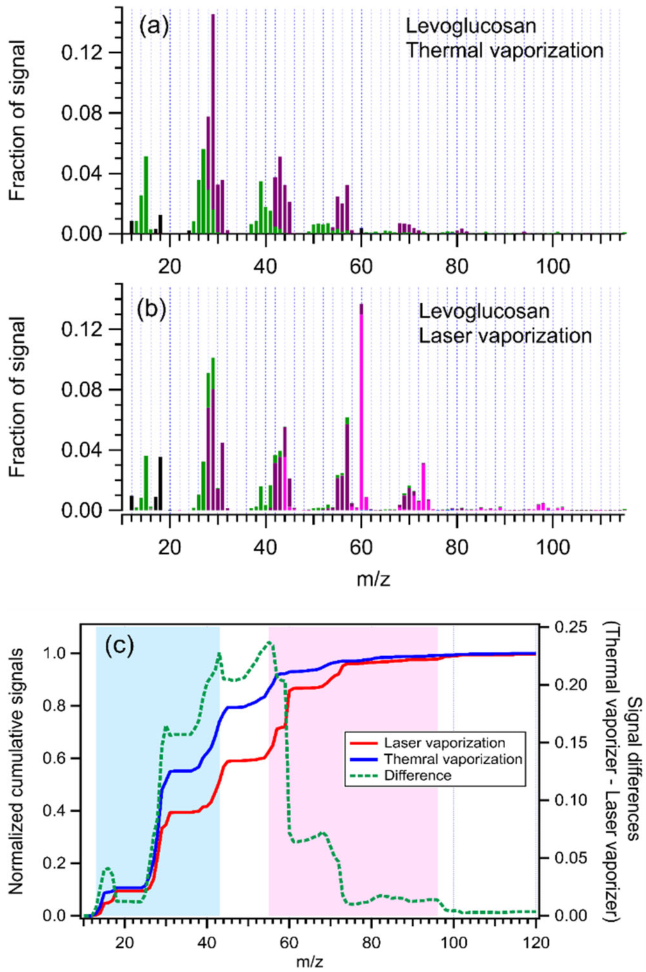

Figure S2. Mass spectra of levoglucosan, measured by the SP-AMS 1 using the tungsten (a) and laser (b) vaporization schemes. (c) Normalized cumulative histogram of mass-to-charge ratios for the oxygenated organic compounds measured by the SP-AMS 1. The blue area indicates that the thermal vaporization scheme tends to provide organic fragments with smaller m/z, whereas the red area indicates that the laser vaporization scheme tends to give organic fragments with larger m/z.

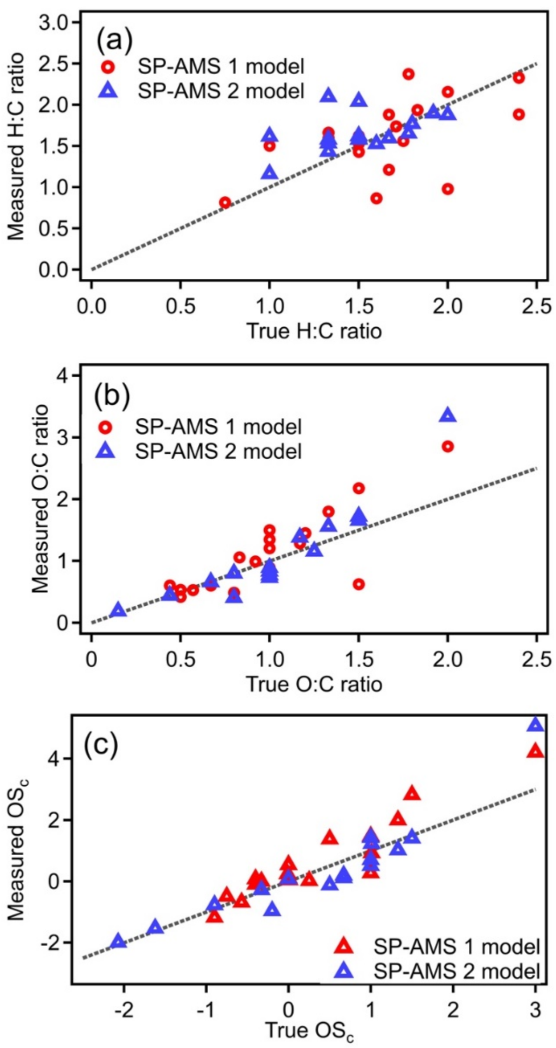

Figure S3. Comparisons between the measured and true values of H:C, O:C, and OSc determined by the two SP-AMS using the laser vaporization scheme. The I-Asp method was used for the elemental analysis. Red circles and blue triangles represent data measured by SP-AMS 1 and 2, respectively. The dashed lines represent 1:1 line.

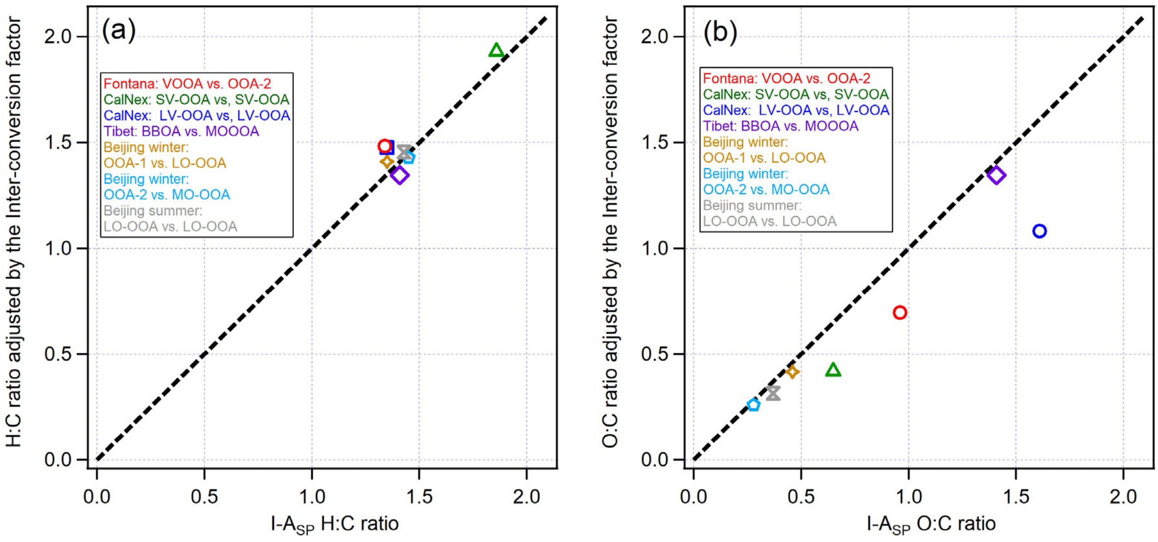

Figure S4. Comparison of elemental ratios determined by the I-A$_{sp}$ method and the I-A method with the inter-conversion factors applied.

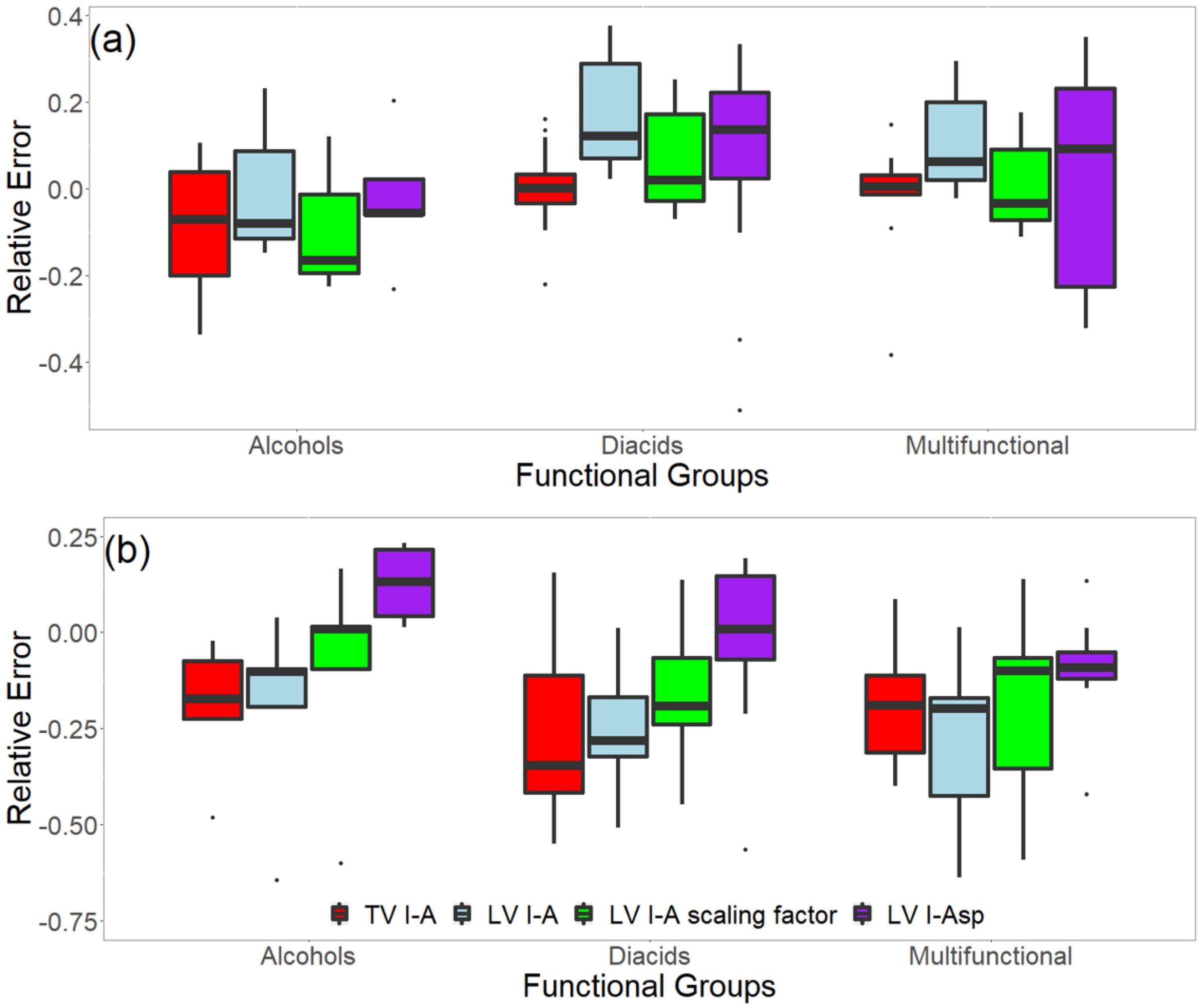

Figure S5. Relative error of H:C (a) and O:C (b) ratios from SP-AMS 1 and 2 calculated with LV and TV methods. TV I-A (red), LV I-A(blue), LV I-A$_{sp}$ (green) and LV I-A scaling factor (purple) are included in the comparison.

Reference

Chen, C. L., Chen, S., Russell, L. M., Liu, J., Price, D. J., Betha, R., Sanchez, K. J., Lee, A. K. Y., Williams, L., Collier, S. C., Zhang, Q., Kumar, A., Kleeman, M. J., Zhang, X., and Cappa, C. D.: Organic Aerosol Particle Chemical Properties Associated With Residential Burning and Fog in Wintertime San Joaquin Valley (Fresno) and With Vehicle and Firework Emissions in Summertime South Coast Air Basin (Fontana), J. Geophys. Res.-Atmos., 123, 10,707-710,731, 2018.

Lee, A. K. Y., Chen, C. L., Liu, J., Price, D. J., Betha, R., Russell, L. M., Zhang, X., and Cappa, C. D.: Formation of secondary organic aerosol coating on black carbon particles near vehicular emissions, Atmos. Chem. Phys., 17, 15055-15067, 2017.

Massoli, P., Onasch, T. B., Cappa, C. D., Nuamaan, I., Hakala, J., Hayden, K., Li, S.-M., Sueper, D. T., Bates, T. S., Quinn, P. K., Jayne, J. T., and Worsnop, D. R.: Characterization of black carbon-containing particles from soot particle aerosol mass spectrometer measurements on the R/VAtlantisduring CalNex 2010, J. Geophys. Res.-Atmos., 120, 2575-2593, 2015.

Wang, J., Liu, D., Ge, X., Wu, Y., Shen, F., Chen, M., Zhao, J., Xie, C., Wang, Q., Xu, W., Zhang, J., Hu, J., Allan, J., Joshi, R., Fu, P., Coe, H., and Sun, Y.: Characterization of black carbon-containing fine particles in Beijing during wintertime, Atmos. Chem. Phys., 19, 447-458, 2019.

Wang, J., Zhang, Q., Chen, M., Collier, S., Zhou, S., Ge, X., Xu, J., Shi, J., Xie, C., Hu, J., Ge, S., Sun, Y., and Coe, H.: First Chemical Characterization of Refractory Black Carbon Aerosols and Associated Coatings over the Tibetan Plateau (4730 m a.s.l), Environ. Sci. Technol., 51, 14072-14082, 2017.

Xie, C., Xu, W., Wang, J., Liu, D., Ge, X., Zhang, Q., Wang, Q., Du, W., Zhao, J., Zhou, W., Li, J., Fu, P., Wang, Z., Worsnop, D., and Sun, Y.: Light absorption enhancement of black carbon in urban Beijing in summer, Atmos. Environ., 213, 499-504, 2019a.

Xie, C., Xu, W., Wang, J., Wang, Q., Liu, D., Tang, G., Chen, P., Du, W., Zhao, J., Zhang, Y., Zhou, W., Han, T., Bian, Q., Li, J., Fu, P., Wang, Z., Ge, X., Allan, J., Coe, H., and Sun, Y.: Vertical characterization of aerosol optical properties and brown carbon in winter in urban Beijing, China, Atmos. Chem. Phys., 19, 165-179, 2019b.

Xu, J., Zhang, Q., Shi, J., Ge, X., Xie, C., Wang, J., Kang, S., Zhang, R., and Wang, Y.: Chemical characteristics of submicron particles at the central Tibetan Plateau: insights from aerosol mass spectrometry, Atmos. Chem. Phys., 18, 427-443, 2018.

Xu, W., Xie, C., Karnezi, E., Zhang, Q., Wang, J., Pandis, S. N., Ge, X., Zhang, J., An, J., Wang, Q., Zhao, J., Du, W., Qiu, Y., Zhou, W., He, Y., Li, Y., Li, J., Fu, P., Wang, Z., Worsnop, D. R., and Sun, Y.: Summertime aerosol volatility measurements in Beijing, China, Atmos. Chem. Phys., 19, 10205-10216, 2019.